Updated: 3 June 2015

Errata and Supplements for the report: "**Polarimetric Upgrades to Improve Rainfall Measurements**; NOAA/NSSL's WSR-88D Radar for Research and Enhancement of Operations; April 1998

Preface to this errata and supplements: The report "**Polarimetric Upgrades to Improve Rainfall Measurements"** has been a useful resource for transferring NSSL research results to the National Weather Service and its contractor Barron Services, Inc. Because the dual polarimetric upgrades have been made by Barron Services to the network of WSR-88D radars at the time of this writing, it seemed useful to update the supplements and errata in case users of the data have interest in reviewing the report to learn the underlying engineering results upon which the upgrades have been based. Furthermore, if there are plans to make measurements of the copolar and cross-polar radiation patterns on KOUN after changes have been made by Barron Services, Inc., this updated report could serve as a baseline. The dual pol upgrades made to KOUN by NSSL were to allow radar meteorologists to thoroughly test over a period of years the performance of the Polarimetric upgrades made to the KOUN before alternative dual pol modifications were made by Barron Services to the fleet of WSR-88Ds. Thus this report and its errata could be useful for comparisons when and if measurements are to be made on the WSR-88D after modifications made by Barron Services.. The errata and supplemental material listed below, a result of the continuing collaboration and exchange between the Radar Operations Center and NSSL should keep this report correct and current.

Page para.   Line

4   2   1   here and every else in the text, change 8.53 m to 8.534 m

        4   ditto, change 0.111 m to 0.1109 m

7 Fig.II.2 (b) caption   change 2nd line to read:"….sidelobe levels with**out** radome."

12   0   6   change to read: '….Thus the scan in Fig.II.4 represents the E plane radiation pattern 0.05^o above the principal plane.'

Fig.II.4(b) caption   at the end of the first line insert "of the antenna without a radome,"

16   1   11   change "might" to "should", and at the end of this paragraph add: "This agreement also suggests that the ad hoc antenna range in Norman is likely suitable for pattern measurements to about the -20 dB level below the radiation peak.

Fig.II.5 caption   revise second line to "….for the NEXRAD antenna without a radome are

given by…"

Fig.II.6   change the label: "calculated aperture illumination" to "calculated illumination on the reflector". Although both labels are correct, this is not proven until p.26. At this point we have only calculated the illumination on the reflector's surface.

25   3   4   change to read: "would be smaller (smaller) than that measured after the change of…."

                6   change to: "…Although this 0.1° difference is small, it is in a direction one would expect…"

             10-12   change the last sentence to read: Moreover, the elevation angle to the radiation source also decreased after the feed change by an about 0.1° (compare…..) as expected if the single port feed was on axis.

25-26 5   change this paragraph to read: "In order to support the deductions that sidelobes along the 0° cut (Fig.II.1a) are principally due to the vertical spar blocking radiation from the aperture, and other anomalous sidelobes are due to scatter from the spars, feedhorn, and imperfections in the parabolic surface , we calculated the sidelobe levels without feed support spars assuming a perfectly made reflector. This calculation gives the radiation pattern outside the ridges of sidelobes due to the feed support spars. We use diffraction theory to compute the ……….. (Sherman 1970)"

26   1   1   change to read: "The dashed line in Fig.II.6 is the calculated illumination of the reflector's surface. This calculation used the feed's radiation pattern adjusted for the changing distance from the feed to points on the surface. The angle between……"

           2   1-4   change to read: "In general the calculation of the actual radiation pattern requires calculation or measurement of the aperture distribution function and numerical analysis. But, we can obtain an estimate of the radiation pattern by fitting the measured *aperture* illumination function, assumed to be circularly symmetric, with an equation for which a theoretical pattern is known. The theoretical pattern is known if the electric field aperture distribution has the general form (Sherman, 1970, pp.9-21):

Eq.II.1 remains the same

2

where ρ is the radial distance…..”

3   because θ in this paragraph is different than θ on p.27, change θ to β everywhere in this paragraph.

3   to clarify the derivation of Eq.(II.2), and to correct an error in computing the secondary radiation pattern, change this paragraph to read:

“The following normalized power density $S_n(\rho)$ (in dB) across the aperture, as derived from (II.1), is

$$S_n(\beta) = 20\log_{10}\left[\frac{\left(1-\rho^2/\rho_o^2\right)^m + b}{1+b}\right] \qquad \text{(II.2a)}$$

To compare this idealized aperture distribution with that calculated from Fig.II.6, we convert the dependence on ρ to one on β by substituting $\rho = (2f/\sin\beta)(1-\cos\beta)$ to obtain

     Equation II.2 is relabeled as (II.2b)

where β is the angle subtended by the line connecting the reflector's vertex to the focus and the line drawn from the focus to a point in the aperture.

     To relate the electric field incident on the surface of the reflector to the aperture illumination function we use the fact that the amplitude of the field at a point 'A' on the reflector's surface is the same as that in the aperture plane at the point which lies on a line passing through point 'A' and parallel to the axis of the reflector (Fradin 1961, p.381). Thus the reflector illumination function (Fig.II.6), calculated from the measured primary radiation pattern, equals the illumination function $S_n(\beta)$ across the aperture. Therefore the radiation intensity given by the dashed line in Fig.II.6 and the power density given by (II.2) are both the aperture illumination functions. The factor raised to the mth power ………
………and its diameter $2\rho_o = 853.4$ cm into (II.2b), we have plotted in a revised Fig.II.6 the theoretical aperture distribution for m = 3 (the fitting was tested for m = 2, 2.5, and 3; m = 3 produced the best fit to the dashed curve in Fig.II.6 over the angular interval $\pm 45^o$. This angular interval is where the illumination is most intense. The curves for m = 2.5 and 2.0 fit the calculated aperture illumination better near the edge of the reflector,

but there the illumination is weakest. It is most important to have the best fit of a theoretical aperture distribution at locations where the illumination is most intense."

27   1   5   change to read: "….patterns (for $m = 3$, and $b = 0.16$) and …."

Eq.II.3   this equation should be revised to:

$$S(u) = 20 \, \mathrm{Log}_{10} \left[5.405 \left| 1.68 \frac{4! J_4(u)}{u^4} + 0.16 \frac{J_1(u)}{u} \right| \right] \qquad (\text{II.3})$$

where

$$u = \frac{2\pi\rho_\mathbf{o} \sin\theta}{\lambda}, \quad 2\rho_\mathbf{o} = 8.534, \quad \lambda(\text{KOUN}) = 0.1109\,\mathrm{m}, \qquad (\text{II.4})$$

and θ is the polar angle measured from the axis of the reflector and a radial to a far field point. This theoretical function ignores changes in sidelobe levels due to spar blockage and reflector surface departure from a parabolic shape. The first term in this equation is the secondary radiation pattern due to the tapered illumination component [i.e., the first term in (II.1)], and the second term is due to the uniform component that illuminates the aperture [i.e., the second term in (II.1)]. The theoretical secondary pattern presented in the revised Fig. II.7 (herein labeled as Fig. II.7a) is computed using a theoretical primary radiation pattern fitted to the measured primary radiation pattern of the dual polarization feed manufactured by Andrew Canada.

27   2   1-2   change to read: "Eq.II.3 is plotted in the revised Fig.II.7 (now Fig.7a) for $0 \le \theta \le 20^\mathbf{o}$ and compared with the envelope of sidelobes (the dashed-dotted line) deduced from a pattern measured by Andrew Canada (Paramax Report, 1992, p. C-6) along the 30° cut. All measurements reported herein were made using linear polarization. The 30° cut was chosen….."

28→29 1, 2   replace these two paragraphs with:

The dashed-dotted line is the eye-balled envelope of the sidelobes on the left side of the pattern (p. C-6; Paramax Report, 1992) for the 30° cut that passes through the region clear of the enhanced sidelobes due to spars. The sidelobe slope is approximately 0.4 dB per degree for sidelobes between 6° and 40° (sidelobes between 20 and 40° are not shown in Fig.II.7a—practically all sidelobes measured by Andrew Canada beyond 20° are below the -55 dB level. Theoretical sidelobe levels beyond 6° are principally due to the second term in (II.3). This is the uniform

4

illumination associated with the illumination of the edge of the dish. The higher is the illumination of the edge, the higher are the far out sidelobe levels.

"Figure II.7a also shows measurements of KOUN's main lobe (i.e., the dots); there is good agreement with the theoretical pattern down to the -15 or -20 dB level. The three data points ($\bullet$) are obtained from KOUN pattern measurements after change of feed [i.e., Fig.II.8(c); a 0° cut]. Antenna range artifacts (i.e., scatter from buildings, terrain, etc.) on NSSL's ad hoc antenna range make it difficult to obtain precise pattern measurements below about -20 dB. Thus subjective estimates of the sidelobe levels as a function of θ are presented as envelopes of the measured patterns that appear to be free of artifacts.
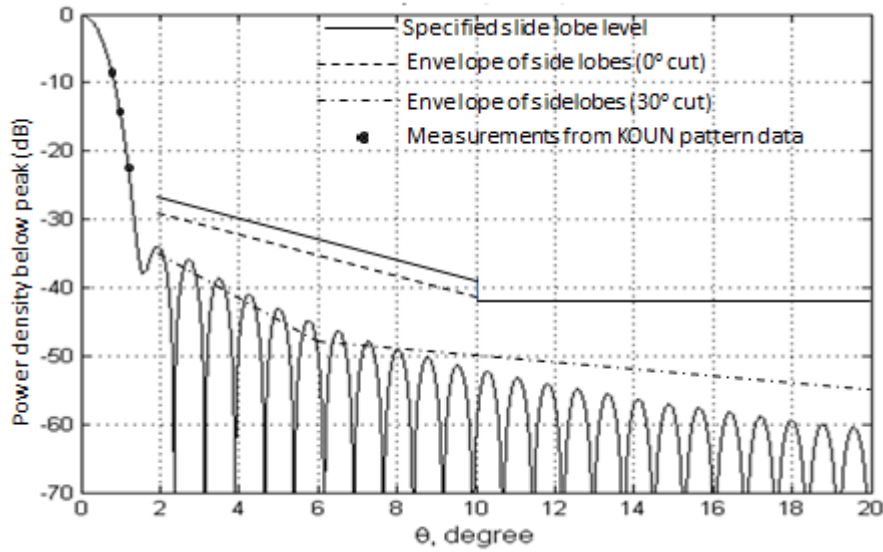

Fig.II.7a KOUN's ($\lambda = 11.09 \, cm$) one-way theoretical copolar radiation pattern (solid wavy line) calculated from (II.3) compared with measurements along various cuts. The dashed line is the envelope of KOUN sidelobes, but the dashed-dotted line is obtained from Andrew Canada pattern data along the 30° cut with the singularly polarized (H) feed and without radome. The solid lines (i.e., -26 to -38 dB for θ from 2° to 10° and at -42 dB thereafter) are those sidelobe limits specified without radome.

The envelope (dashed line) of measured side lobes for KOUN with radome and along the 0° cut after change of feed is from Fig. II.8(b); this cut passes through the ridge of enhanced sidelobes due to spar blockage

5

(this is the only cut through the main lobe peak that can be made for KOUN). This envelope is obtained from the right side of Fig. II.8(b) and connects the tops of the 2 highest sidelobes in the angular interval between 2° and 10°; the left side sidelobes are even lower. Thus all KOUN sidelobes in the interval from 2° to 10° for the 0° cut fall below the dashed curve! Admittedly these measurements are subject to significant error due to the ad hoc NSSL antenna range, but they provide an approximate measure of the sidelobe levels along the three ridges of enhanced sidelobe due to the three feed support spars.

Returning to the discussion of the dashed dotted lines in Fig.II.7a, the 30° cut sidelobe level of the center-fed WSR-88D reflector is practically the same as that obtained for an offset-fed reflector that has no blockage associated with feed support spars (compare Fig.II.7a with Fig.7 of Bringi, et al., JTECH. 2011). Thus the most significant advantage of the offset parabolic reflector is the lack of a ridge of sidelobes due to spars blocking secondary radiation. These heightened levels of sidelobes can cause meteorological measurement error if the ridge of sidelobes illuminates regions of significantly enhanced reflectivity.

Although the envelope of sidelobes for the 30° cut was measured by Andrew Canada—the NSSL antenna range is not designed to make pattern measurements along cuts other than the 0° cut—for a WSR-88D antenna without radome and with the feed generating H linearly polarized radiation, the Andrew Canada sidelobe "pattern" is also representative of the KOUN sidelobe "pattern" with radome and using the dual polarized feed. That is, it is assumed the randomly located seams of the WSR-88D radome principally decreases the gain, but does significantly alter the pattern in selective directions as seen with a radome that has a periodic structure (e.g., Fig.7.26 of Doviak and Zrnic, 2006; the radome induced sidelobes lie along the line $\pm30^o$ from the $\theta_e = 0^o$ line).

That sidelobes of KOUN beyond 20° are below -55 dB is supported by KOUN pattern data presented in Fig.II.4a for the 0° cut; a worst case cut. Thus, we conclude the KOUN sidelobes outside the narrow angular regions of enhanced sidelobes due to struts has a first sidelobe at about -35 dB at 2°, and sidelobe levels decrease linearly in dB to about-48 dB at 6°, and again decrease at a slower rate to about -55 dB at 20°.

Sidelobes measured for KOUN are a few dB higher than those 0° cut measurement on the right side of the pattern on page C-4 of the Paramax Services Corp., 1992 report—i.e., Paramax, 1992. The pattern measurements on page C-4 were made at the Andrew Canada range for another WSR-88D reflector without a radome whereas the KOUN measurements were made with a radome. The measured KOUN sidelobe level increase over that seen from Andrew Canada's data is partly due to the radome (Sections II.1.1 and II.1.2.4), but also likely to the less-than-

6

ideal antenna range used for the KOUN measurements. We therefore conclude the KOUN sidelobe levels after installation of Andrew Canada's dual-pol feed horn is the same as that measured by Andrew Canada on a WSR-88D antenna when a single-pol feed horn illuminated the antenna's reflector. This conclusion is reasonable and supported by the fact the dual-pol feed is identical to the single-pol feed except an extra port has been added----no change had been made to the conical waveguide and aperture of the feed horn.

The solid lines are the allowed worse case sidelobe levels specified for the antenna **without radome.** These specified levels were given to Andrew Canada (Paramax, 1992), and are 2 dB lower than specified by the NTR for a WSR-88D with radome. The envelope of the ridge of measured KOUN sidelobes (dashed line) due to spars and radome fall below this specified value, but is considerably higher than the theoretical ones that ignore beam blockage from the spars and feed horn, radome effects, and perturbations of the reflector's surface.

There are three ridges of heightened sidelobes (dashed lines in Fig. II.1a show the locations of the ridges), and each ridge is estimated to have an azimuthal width of about 2°.The significant enhancement of sidelobes due to spar blockage is also clearly seen in the CSU data (i.e., Fig. II.5a). Moreover, Raytheon has made 2D pattern measurements that clearly shows the ridge of enhanced sidelobes due to three feed horn support struts that block radiation from a WSR-88D reflector (Fig.II.7b—this figure is from a Raytheon Report. We have received selected pages of this report from, I believe NWS/ROC, but we were unsuccessful in finding the full report).

Each of the WSR-88D struts extends from the rim of the reflector to the feed horn which is on the axis of the reflector. Because there are 3 struts on the WSR-88D ante*n*na, there are three ridges of sidelobes each passing through the origin (i.e., the beam axis)—thus there are 6 half-length ridges of sidelobes emanating from the origin and they are spaced 60° apart.   Each of the 3 ridges of sidelobes is perpendicular to the strut that causes the ridge of sidelobes. These sidelobe ridges are labeled in the figure as "strut sidelobes", and we assume this to be associated with blockage of the radiation from the reflector. In Andrew Canada measurements the antenna is set in a normal configuration (i.e., as it would be for the operational WSR-88D) whereby one of the three struts is vertical. In this configuration the ridges of sidelobes appear along lines of constant azimuth (i. e, they appear straight). But for the measurements made by Raytheon, the antenna was rotated ccw 15° thus causing the ridges of sidelobes to be curved as seen in Fig.II.7b.

NEXRAD S-BAND ANTENNA
2-D FAR FIELD PATTERN

F = 2.85 GHZ

BACKSCATTER
LOBES

MAIN BEAM (IN CENTER)

0° ELEVATION

-10° ELEVATION

STRUT
SIDELOBES

-10° AZIMUTH   10° AZIMUTH

13

Fig.II.7b The two dimensional radiation pattern of a NEXRAD antenna
fabricated by Raytheon Corp.

An unexpected feature of the Raytheon 2D radiation pattern is the
additional three sidelobe ridges Raytheon identifies as "backscatter lobes".
No explanation is provided in the few pages of the report that was given to
us. Nevertheless, because the number of "backscatter lobes" is three and
the ridge is aligned with each of the struts, it seems likely these
"backscatter lobes" are an inherent property of the antenna, and not an
artifact of the antenna measuring range. Similar ridges of sidelobes
emanating at azimuths aligned with the spar directions is seen in other
pattern measurements (Rusch, et al., 1982[1], and Hartsuijker, et al, 1972[2]).

---

[1] Rusch, W. V. T., O. Sorenson, and J. W. M. Baars, 1982: Radiation Cones from Feed Support Struts of
Symmetrical Paraboloidal Antennas, IEEE Trans. Antenna and Prop., AP-30, No. 4, 786-790.
[2] Hartsuijker, A. P., J. W. M. Baars, S. Drenth, and L. Gelato-Volders, 1972: Interferometric Measurements of
paraboloidal antenna at Dwingeloo radio observatory, IEEE Trans. Antennas and Prop., AP-20, 2, 166-176

Moreover, another look at Andrew Canada's pattern measurements along the 30° and 90° cuts (the 90° cut is a vertical cut and one spar lies in the vertical plane) show on one side of the mainlobe an enhanced ridge of sidelobes consistent with the Raytheon measurements. An example of the radiation pattern along the vertical cut is given as Fig.7.28 in the Doviak and Zrnić (1993; however the abscissa of Fig.7.28 is incorrectly label in the book as azimuth, it should be elevation).

From the 2D pattern, it is difficult to estimate the intensity of the three ridges of "backscatter lobes". Thus we have examined Andrew Canada's plots for the 30° and 90° cuts and found the "backscatter lobes" have intensities about 40 and more decibels below the peak of the mainlobe (e.g., Fig.7.28 at negative elevation angles). If these estimates derived from the Andrew Canada data apply to the WSR-88D antennas, then the contribution from "backscatter lobes" will be less than that from the enhanced ridge of sidelobes due to blockage of aperture radiation.

| 29 | 1 | 1-9 |

change to read: "The following formula

$$\theta_1 \simeq 1.27 \frac{\lambda}{D} \, (\text{rad.}) \,. \tag{II.5}$$

fits well the one-way beamwidth measurements and the beamwidth obtained from the theoretical radiation pattern (i.e., 0.946° from (II.5) and 0.95° from the theoretical radiation pattern. Although this formula applies well for KOUN at the wavelength of 11.09 cm, this theoretical expression also applies well for the WSR-88Ds operating in the band 11.11 to 10 cm (i.e., 2.7 to 3.0 GHz). For example at $\lambda = 10$ cm (II.5) gives $\theta_1 = 0.853°$; this compares reasonably well with 0.85° measured by Andrew Canada (Paramax, 1992 pp. C-55, C-57). The Andrew Canada reported beamwidth measurements (i.e., for horizontally polarized waves; the feed used in the legacy radar transmitted only H polarized waves) at each of the selected wavelengths are an average of five measurements made at different cuts across the beam.

Furthermore, measurements made by Seavey Engineering (Barron Radar, 2009, p.22), in 2009 on another WSR-88D reflector illuminated with 11.11 cm H radiation from another dual polarimetric feed gives a beam width of 0.95°, also in good agreement with that derived from the formula. However, Seavey measurements are subject to more error because they are widths obtained from one pattern cut. Moreover, because feed horns are different, there is no expectation that the beamwidths

measured by Seavey Engineering should be in exact agreement with those measured by Andrew Canada. Nevertheless, based upon the few available data, the theoretical formula $\theta_1 = 1.27\lambda / D_a$ appears to provide, for the WSR-88D antennas, beamwidths with accuracy better than 0.1^o over the entire operating band of frequencies.

The angular diameter θ_0 of the first null circle (the first null circle is a minimum not a zero) obtained from Fig.II.7a for KOUN is 3.1^o. The good agreement of the half power beam width formula for operation in the entire band suggests that the angular diameter of the first null for other WSR-88D radars can be obtained from the formula

$$\theta_0 = 4.16\frac{\lambda}{D}\text{(rad)} \tag{II.6}$$

The angular diameter of the first null circle defines the main lobe or beam of the antenna. Substituting into (II.6) gives $\theta_0 = 3.10^o$ for KOUN. Comparing with that 3.45^o measured by Andrew Canada [i.e., Fig.II.2(b) right panel] and that measured by NSSL for KOUN [i.e., 3.56^o from Fig.II.8(c)], it is seen both independent measurements agree to within 0.1 dB, but differ significantly from the 3.1^o obtained from (II.6). The measured null location is subject to significant error because the antenna range is not ideal (i.e., measurements more than 20 dB below the main lobe peak are subject to significant errors induced by scatterers on the antenna range). However the null circle diameter obtained from II.6 is in excellent agreement with the theoretical value of 3.12^o obtained by interpolating data in Table 2 of Sherman (1970).

	2		delete this paragraph because it no longer applies to the revised Eq.II.3.
32	1	6-8	change 1.04^o to 0.95^o and delete the last sentence.
34	3	2	change to read: "…illustrates that the cross-polar radiation along the…"
		9	add: (4) reflection of the copolar beam from the ground and conversion of H polarization to V polarization (and vice versa) from scatterers on the ground.
36	1		at the end of this paragraph add: For example, if the cross-polar and copolar fields are in or out of phase, a null in the on axis radiation would be achieved by rotating the

10

source antenna by $\frac{\pi}{2} \pm \tan^{-1}(E_{xp} / E_{cp})$ where E_{xp} and E_{cp} are the cross-polar and copolar field amplitudes along the boresight. Thus a -32 dB on-axis cross-polar peak could be nulled by a 1.4^o tilt of the source antenna, a sufficiently small angle that it might not be noticed by eye. If the cross-polar and copolar were in phase quadrature, a minimum in signal having the magnitude of the cross-polar radiation would be observed. Thus nulling the cross-polar radiation by rotating the source antenna requires measurements of its orientation to insure that nearly pure H and V radiation is transmitted or received along the beam axis. Precise orientation measurements would verify whether the antenna under test is transmitting and receiving nearly pure H and V radiation along the beam axis.

37   at the top of this page insert the following paragraph:

To support the contention that an on-axis peak of cross-polar radiation could exist for the WSR-88D (and perhaps for the CSU antenna), we refer to the work of Potter (1963)[3]. Potter states that in order to obtain circularly symmetric beams for both the H and V polarized waves from a circularly symmetric feed, a TM_{11} mode should be excited within the throat of the feed. Potter presents radiation patterns of this feed showing excellent symmetry of the copolar radiation pattern. On the other hand, there also is a pronounced on-axis peak in the cross-polar radiation! This peak in cross-polar radiation is about 33 dB below the copolar peak, in remarkable agreement with the WSR-88D cross-polar peak observed in Fig. II.6. It is therefore suggested that the cross-polar peak could be due to a purposely excited TM_{11} mode in the throat of the WSR-88D feed, and not necessarily conversion to cross-polar radiation upon reflection of the copolar beam from the ground. Unfortunately we do not have any evidence that a TM_{11} mode was or was not excited in the WSR-88D feed horn.

1   delete the first sentence **and last** sentence and modify the paragraph to "Comparing the CSU and WSR-88D… beyond $\pm 9^o$, so we are unable to make comparisons of levels far removed from the main lobe. The significantly higher sidelobe levels of the CSU antenna are simply due to the fact that these higher sidelobes are along a ridge of sidelobes due to spar blockage whereas the WSR-88D radiation field does not have a ridge of enhanced sidelobes along the 45° cut."

---

[3] Potter, P. D., 1963: A new horn antenna with suppressed sidelobes and equal beamwidths. *The Microwave Journal,* June, pp. 71-78.

On the other hand, measurements presented by Chandrasekar and Keeler (JTECH, 1993) of copolar fields along a cut between the four struts of NCAR's CP-2 10 cm weather radar show sidelobes to be not significantly lower than along the cuts that contain the ridge of enhanced sidelobe levels due to the spars (compare Figs 4 and 8). This observation suggests that the cause of sidelobes of NCAR's and CSU's antenna being significantly higher than those of the WSR-88D is not associated with struts, but perhaps is rooted in the design of the feed horn, or the poor performance of their ad hoc antenna range.

	2		last line: Change II.6.4 to II.6.7.
39	1	1	change "Section II.3" to "Section II.6.2"
40	2		at the end of this paragraph add: On the other hand, because the antenna range is not ideal, achieving a null by rotating the standard gain horn does not necessarily imply that the null is a characteristic of the cross-polar pattern as discussed in the next paragraph,
41	0	6	change "less" to "more"
		7-8	change to: "…a few dB below this level (i.e., -33 dB) could also be in error as mentioned in Sections II.6.5 and II.6.7. Thus it is not surprising that KOUN's copolar sidelobes…."
	0		at the end of this paragraph add: "To obtain better measurements of the cross-polar fields, we made additional measurements described in Section II.6.7.
42	2	4	change "Section II.6.7" to "Section II.6.6"
44	1	2	(Figs.II.13a, b) should be (Figs.II.11a, b).
46	1	5	insert after "…dB level.": The significant differences at azimuths larger than plus/minus 1° could be due to scatter from artifacts (i.e., buildings, utility poles, tress, etc.) associated with the antenna range in Norman,. Also, bear in mind…"
		10	change to: "…scan for the 0° elevation cut are more likely…
		11	delete this last line.
46			the equation should be placed after the second line of the third paragraph

49	2	1	change to read: "Cross-polar radiation (e.g., A_v) combines with copolar radiation (e.g., A_H) to form, in general, …."
		9	change to: "….(Fig.II.A.1 in which the ellipse collapses to a line for linear polarization). τ is positive…"
	3	1	change to: "..between the vertical (cross-polar) and the horizontal (copolar) fields is not 0…"
	Eq (II.8)		the equality symbol should be replaced by an approximation symbol.
		5	change to: "….Appendix (i.e., Section II.8)…"
		6	delete the parenthetical phrase.
		7	change "receiver" to "transmitter".
50	2	3	change to: "…The standard gain horn, transmitting H or V polarized waves, was rotated until a minimum was established in the KOUN's V or H receive channel. That a minimum was achieved and not a zero (i.e., not a sharp and deep null) suggests the cross-polar field is in phase quadrature to the on-axis copolar field. The amount of …."
	Fig.II.A.1		replace E_{vo} and E_{Ho} respectively with A_v and A_H.
55	3	4	change to: ....which RHC (or LHC) was chosen for transmission and LHC (or RHC) was chosen for reception....
56	Eq.(III.1)		for modifications to this equation if the antenna transmits both copolar and cross-polar waves , see Supplements on pages 240-241 in the errata to the book "Doppler Radar and Weather Observations" Academic Press, 1993. These errata are periodically updated and posted on NSSL's website at www.nssl.noaa.gov. In the "Quick Links" box select "Publications" to open the page to select "Recent Books" to find the book and listed Errata for the 3rd and 4th printings.
57	0	5	change "polarizabilities" to "susceptibilities".
		11-12	modify these lines to read: ".... the wave normal $\boldsymbol{k}$, the apparent canting angle ψ, the true canting angle ψ', and δ ."
	1	12	change to read:....because $4\pi<|s_{hh}|^2> \equiv \sigma_b$ (McCormick and Hendry, 1975),

it is seen...."

58   0   1   change to read: "......scatterer's properties **X.**"

61   4   5   last line change to: "….the incident field. Canting angles are…"

62   0   8-9   modify to read: "ϕ_{DP} (radians) is the phase difference between the scattered H and V waves at the antenna in absence of canting angle dispersion σ_ψ^2 (radians), and assumes that the phase……… ℓ_{hv} ($\ell_{hv} > 1$) is …*power* loss factor"

    1   1   change to: "The transformation matrix $\boldsymbol{V}^{(\mathrm{T})}$, which relates…"

          2   change to: "….[E$_{\mathrm{th}}$, E$_{\mathrm{tv}}$] as it leaves the antenna to the polarization state of the scattered field vector [E$_{\mathrm{rh}}$, E$_{\mathrm{rv}}$] returned to the antenna, is,

(III.22)   delete the first matrix.

After (III.22) insert:
    In the balance of section III.1 it is assumed H, V waves are alternately transmitted, but simultaneously received (i.e., the ATSR mode). Assuming there is no cross-coupling within the antenna (i.e., the antenna does not transmit or receive cross-polar fields) and the transmitted field intensities with horizontal or vertical polarization are equal, the normalized signals received are:

$$\begin{bmatrix} V_{\mathbf{rh}} \\ V_{\mathbf{rv}} \end{bmatrix} = \boldsymbol{V}^{(\mathrm{T})} \begin{bmatrix} 1 \\ 0 \end{bmatrix} \text{ or } \boldsymbol{V}^{(\mathrm{T})} \begin{bmatrix} 0 \\ 1 \end{bmatrix}$$

in which the normalized transmitted E_{th} (i.e., $\vec{E}_t^{(\mathrm{h})} = [1, 0]$) and E_{tv} are assumed to have unit amplitudes. Thus voltages [V_{rh}, V_{rv}] received in the H and V channels are alternately copolar and cross polar. The copolar echoes are used to compute $\tilde{Z}_{\mathrm{dr}}$, the observed differential reflectivity, and the cross-polar echoes are used to compute $\tilde{L}dr_{\mathrm{vh}}$, the observed linear depolarization ratio.

(III.23)   Modify (III.23) to read as

$$\tilde{Z}_{dr} \equiv \frac{\langle | V_{\mathrm{rh}}^{(\mathrm{h})} |^2 \rangle}{\langle | V_{\mathrm{rv}}^{(\mathrm{v})} |^2 \rangle} = \text{.......} \tag{III.23}$$

where $\langle |V_{\text{rh}}^{(h)}|^2 \rangle$ is proportional to the mean echo power received in the H channel when the H transmit port is excited (i.e., $\langle |V_{\text{rh}}^{(h)}|^2 \rangle$ is the copolar echo power), and $\langle |V_{\text{rv}}^{(v)}|^2 \rangle$ is the mean echo power received in the V channel when the V transmit port is excited, Z_{dr} is the intrinsic…….

.

		8	change to: "..resolution volume), and the diacritical tilde (~) denotes a measured parameter."
		9	change to: "…..transmission loss factor. In stratified…."
63	1	1	change $\tilde{LDR}_{\text{vh}}$ to $\tilde{Ldr}_{vh}$
64	0	1	change to read: ...a column vector $[E_r, E_l]^t$ of the circularly polarized....
		2	change to read: ....is the column vector $[E_h, E_v]^t$ for linearly polarized waves, and....
	Eq.III.28		the first and last matrices of this equation should be

$$\begin{bmatrix} 1 & -j \\ 1 & j \end{bmatrix} \quad\cdots\cdots\cdots\quad \begin{bmatrix} 1 & 1 \\ -j & j \end{bmatrix}$$

	Eq.III.29		the signs of 'j' need to be changed
65	Eq.III.31		sign of 'j' needs to be changed (note the polarity of 'j' in Eqs.30 and 31 are opposite to that used by Torlaschi and Holt in order to be consistent with the convention chosen in our report)
	2	2	change III.3.0 to III.30
	Eq.III.32		sign of 'j' in the lower of the two equations needs to be changed
	2	5	delete "a solution valid even if drops are not equi-oriented"
	Eq.III.33		the 'j' sign multiplying φ_{DP} needs to be +, and $<s_{hh}s_{vv}^*>$ should be $<s_{hh}^* s_{vv}>$.
66	1	1	Change III.3.3 to III.33
	Eqs.III.34, 35		make the same changes as done for Eq.III.33
	1	13	change III.3.5 to III.35

			the sign multiplying the *Real part* in the numerator needs to be +
	Eq.III.36		
	3	5	change to read: ....., which is often the product of....
67	2	7	change copolar to cross-polar
70	1	8	delete "linear"
83	2	3	modify to read:......and that all drops are of the same size and shape, and that they do not vibrate nor are they canted within
84	0	9	change to read: Because all drops are identical, the V_h'......
94	Fig. IV.7		change caption to read: .....Z_{DR} varies from -1 to +3 dB in the ....
95	2	2	change Z_{DP} to K_{DP} at both places
98	Eq.IV.29		change $\left|\rho_{hvm}\right|$ to $\left|\rho_{hvm}(0)\right|$ and ρ_{hv} to $\left|\rho_{hv}(0)\right|$
	1	1	change $\left|\rho_{hvm}\right|$ to $\left|\rho_{hvm}(0)\right|$
		2	change ρ_{hv} to $\left|\rho_{hv}(0)\right|$; delete $\left|\rho_{hv}(0)\right|$ at the beginning of the sentence and change to read: This bias, obtained from (IV.29), is plotted.....
98-100	last line		change to read: ...the added change in K_{DP} would be about 0.03^{o} km^{-1}...
100	1	7-8	change to read:......the capability to simultaneously transmit H, V waves, but to alternately receive the reflected H, V waves in a single receiver through the use of a low power switch; this mode of operation......
101	Fig. IV.12		labels on some of these figures are incorrect. The dimension of K_{DP} is degree per km; ρ_{hv} has no dimension, and Z_{DR} has dimensions of dB.
List of References			Insert: Potter, P. D., 1963: A new horn antenna with suppressed sidelobes and equal beamwidths. *The Microwave Journal,* June, pp. 71-78.